Drug Design, Development and Therapy

Dovepress
open access to scientific and medical research

Open Access Full Text Article

ORIGINAL RESEARCH

Integrating Network Pharmacology, Molecular Docking and Pharmacological Evaluation for Exploring the *Polyrhachis vicina* Rogers in Ameliorating Depression

Junhui He[1,*], Dongbo Han[2,*], Chunlian Jia[2,*], Jiaxiu Xie[1], Fucui Zhu[2], Jie Wei[1], Dongmei Li[1], Dongmei Wei[1], Yi Li[1], Li Tang[3], Guining Wei[1,4], Jing Yan[4], Yuanming Tong[1], Lifang Yang[4,*], Xuecai Tan[4,*]

[1]Department of Pharmacology, Key Laboratory of Quality Standards, Guangxi Institute of Chinese Medicine & Pharmaceutical Science, Nanning, 530022, People's Republic of China; [2]Department of Pharmacology, Guangxi Medical University, Nanning, 530021, People's Republic of China; [3]Department of Pharmacy, the First Affiliated Hospital of Guangxi University of Traditional Chinese Medicine, Nanning, 530022, People's Republic of China; [4]Guangxi Key Laboratory of Chemistry and Engineering of Forest Products, School of Chemistry and Chemical Engineering, Guangxi Minzu University, Nanning, 530008, People's Republic of China

*These authors contributed equally to this work

Correspondence: Xuecai Tan; Lifang Yang, Guangxi Key Laboratory of Chemistry and Engineering of Forest Products, School of Chemistry and Chemical Engineering, Guangxi Minzu University, Nanning, 530008, People's Republic of China, Tel +86 0771-5877473, Email gxunxctan@126.com; yanglf1990@163.com

Purpose: To investigate the mechanisms of antidepressant action of active fraction of *Polyrhachis vicina* Rogers (AFPR) through network pharmacology, molecular docking and experimental validation.

Methods: GC-MS was used to predict chemical compounds, corresponding databases were used to predict chemical compound targets and depression targets, Cytoscape software was used to construct and analyze the protein interaction network map, DAVID database was used to analyze gene ontology (GO) and KEGG signaling pathway, and AGFR software was used to perform molecular docking. Subsequently, the underlying action mechanisms of AFPR on depression predicted by network pharmacology analyses were experimentally validated in a CORT-induced depression model in vitro and in vivo.

Results: A total of 52 potential targets of AFPR on antidepressant were obtained. GO is mainly related to chemical synaptic transmission, signal transduction and others. KEGG signaling pathways are mainly related to cAMP signaling pathway and C-type lectin receptor signaling pathway. The experiment results showed that AFPR significantly increased the expression of PRKACA, CREB and BDNF in mouse brain tissue and PC12 cells. Furthermore, after interfered of cAMP in PC12 cells, the decreased expression of PRKACA, CREB and BDNF was reversed by AFPR.

Conclusion: AFPR may exert antidepressant effects through multiple components, targets and pathways. Furthermore, it could improve neuroplasticity via the cAMP signaling pathway to improve depression-like symptoms.

Keywords: PC12 cells, BDNF, corticosterone, CAMP signaling pathway, GC-MS

Introduction

Major depressive disorder (MDD) is a very common mental disorder affecting more than 4.4% of the world's population.[1] Over the years, the number of people with depression has increased dramatically due to the ravages of the new coronavirus. MDD, characterized by lack of pleasure, lack of motivation, pessimism and self-blame, with suicidal tendencies in severe cases, is a devastating mental illness.[2,3] Approximately 850,000 tragedies occur due to depression every year,[4] while available, rapid, potent and sustained clinical antidepressants are in shortage. In recent years, the role of Chinese medicine in the field of antidepressants has become increasingly prominent, and several studies have shown that Chinese medicine can regulate the development of depression.[5–7]

Received: 14 December 2022
Accepted: 12 February 2023
Published: 9 March 2023

Graphical Abstract

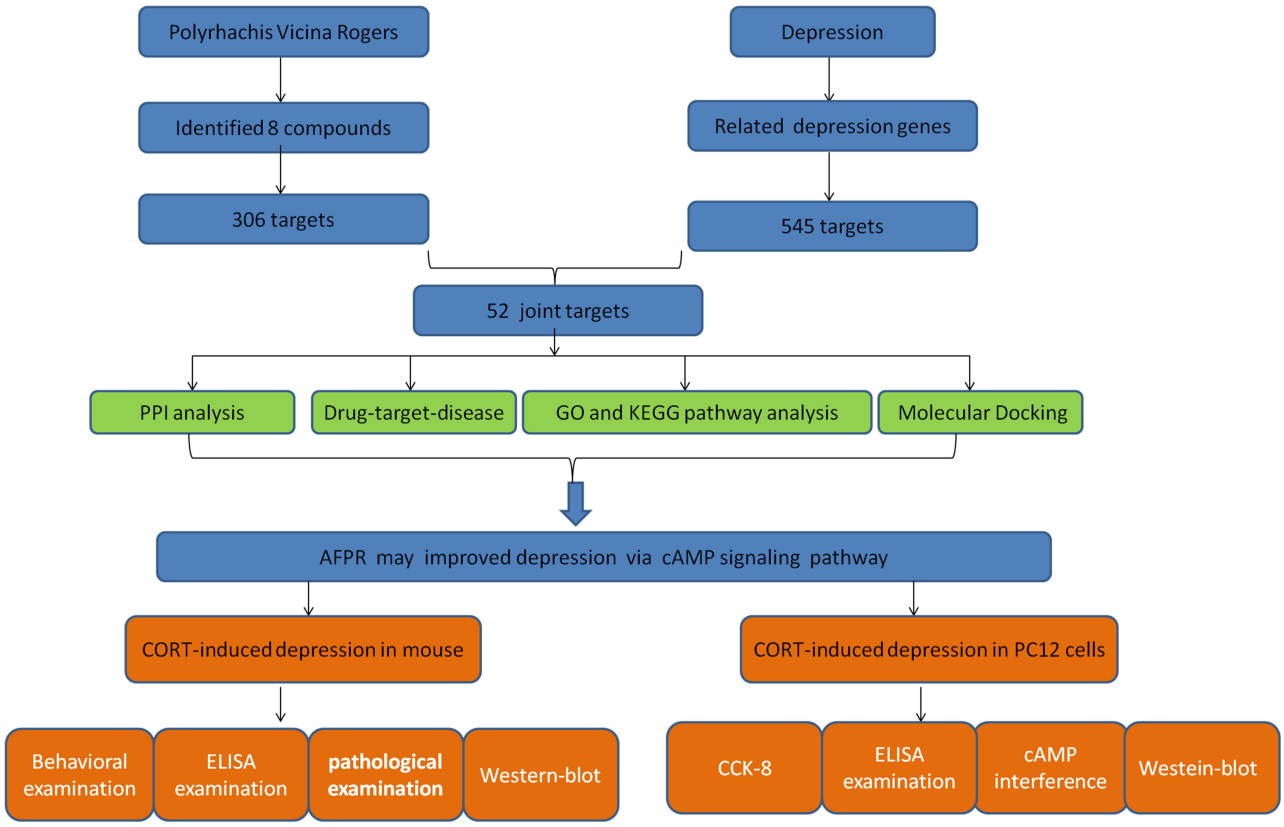

The *Polyrhachis vicina* Roger is a common TCM, with the efficacy of tonifying the kidney and benefiting the essence, invigorating the meridians, detoxifying and eliminating swelling, etc. In clinical, it is mainly used for neurasthenia, insomnia, hemorrhoids, alopecia, rheumatic paralysis and other diseases.[8] Furthermore, the medicine is an insect herb for both medicinal and food use, which contains a variety of amino acids, vitamins and trace elements. The most widely used dosage form is wine, which is mainly used for preventive health care or treatment of rheumatoid arthritis and other diseases. Our previous studies have shown that AFPR have obvious antidepressant effects, but the underlying mechanism remains to be elucidated.

In recent years, network pharmacology has become a powerful tool for TCM research as it allows researchers to study the mechanism of action of compounds from the molecular level to the pathway level.[9] According to the characteristics of multi-component, multi-target and multi-pathway synergy in traditional Chinese medicine, network pharmacology has changed the model of "one target, one drug" into a new model of "multi-target, multi-component", and elucidated the complex interactions among genes, proteins and metabolites related to diseases and drugs from the perspective of network.[10,11] This newly emerging TCM study method has been widely used in the treatment of cancer, asthma and cardiovascular disorders.[12] The newly research has found that the method could also be used in the treatment of other diseases, such as depression,[13] Alzheimer's,[14] etc.

In the current study, network pharmacology was used to analyze the AFPR at a holistic level and found that it could improve depression by regulating the cAMP signaling pathway. Interestingly, CREB and BDNF—key targets in the cAMP signaling pathway—are key targets that affect neuroplastic function, which is closely linked to depression. In recent years, exploring the mechanism of action of depression based on the function of neuroplasticity has become a hot topic of scientific research. In order to verify whether AFPR regulate neuroplasticity through cAMP signaling pathway to

improve depression-like symptoms, this study was proposed to investigate the antidepressant effects of AFPR at the in vitro and in vivo level using a CORT-induced depression model, respectively. After confirming the regulatory effect of AFPR on the cAMP pathway, cAMP was interfered to detect the expression of key proteins in the pathway to provide experimental proof for verifying that AFPR ameliorates depression through the cAMP pathway and to provide new experimental basis and research ideas for the application of AFPR in depression.

Materials and Methods

Reagents

Dried *Polyrhachis vicina* Rogers were purchased from Nanning Zhenyuan Biotechnology Co., LTD (Nanning, Guangxi, China). DA, 5-HT, NE, BDNF and β-NGF assay kits were purchased from Shanghai Fanke Industrial Co., LTD. (Shanghai, China). Toluidine blue dye was purchased from Wuhan Xavier Biotechnology Co., LTD. (Wuhan, China). Hematoxylin–eosin (HE) staining solution was purchased from Beijing Regen Biotechnology Co., LTD. (China, Beijing). PRKACA, CREB and BDNF were purchased from Wuhan Sanying Biotechnology Co., LTD. (Wuhan, China). P-CREB was purchased from Abcam company (USA). Corticosterone (CORT) was provided by Aladdin (Shanghai, China).

Drug Preparation

The crushed *Polyrhachis vicina* Rogers (1000 g) was soaked in 95% ethanol and extracted for 3 times with water bath in a reflux system, the filtrate was collected and concentrated, then extracted with petroleum ether, and the upper liquid was collected and concentrated into a thick paste (56.23 g). A total of 4.5 g paste was emulsified with 100 mL 2.0% Tween-80 to obtain the active fraction of *Polyrhachis vicina* Rogers (AFPR).[15–17]

Chemical Composition Analysis of AFPR

GC-MS was used to predict the chemical composition of AFPR. GC conditions were 120 °C, 1 min; 5 °C/min, 150 °C, 0 min; 3 °C/min, 260 °C, 2 min; 20 °C/min, 280 °C, 3 min; injection volume: 1 μL; split ratio: 50:1; carrier gas: high-purity helium; flow rate: constant flow 1 mL/min. MS conditions were inlet temperature 230 °C; transmission line temperature 240 °C; ion source temperature 230 °C; quadrupole temperature 150 °C; collision gas 1.5; quenching flow rate 2.25; scan range 35–500; solvent delay 5 min; collision energy 70 eV. The data were used NIST 17 database to analyze.

The Construction of Drug Compound Targets and Depression Targets

The databases of Swiss Target Prediction (http://www.swisstargetprediction.ch/) (screening condition is Probability >0) and Integrative Pharmacology-based Research Platform of Traditional Chinese Medicine (TCMIP) (http://www.tcmip.cn/TCMIP/index.php/Home/Login/login.html) (the screening criterion was similarity threshold ≥0.6) were used to predict and construct the compound target libraries. The databases of TCMIP, GeneCards (http://www.genecards.org/), HPO (https://hpo.jax.org/app/), OMIM (https://www.omim.org/) and DrugBank (https://go. drugbank.com/) were used to predict and construct depression target libraries and then remove duplicate targets after aggregation.

The Intersection of Drug Component Targets and Depression Targets

The online Venn diagram website (http://bioinformatics.psb.ugent.be/webtools/Venn/) was used to construct the intersection of drug component targets and depression targets, which was the potential antidepressant target of AFPR.

Protein–Protein Interaction (PPI) Network Analysis

The above intersection targets via the STRING (https://cn.string-db.org/) website to draw the PPI network maps, then the PPI network file was imported into Cytoscape software to analyze the network feature values. The network nodes with Degree values >1.5 times the median were screened as key network targets (or Hub nodes) for AFPR treatment of depression, and the Hub nodes were used to analyze GO and KEGG pathway.

GO and KEGG Signaling Pathway Analysis

The above Hub nodes were used to analyze GO and KEGG pathway through the DAVID (https://david.ncifcrf.gov/) website. Then, the p-values were sorted from smallest to largest, and the top 10 with $P < 0.01$ were selected for GO analysis and the top 20 for KEGG analysis. The microbiology letter website (http://www.bioinformatics.com.cn/) was used to draw the GO and KEGG graphs.

Molecular Docking

The chemical components and Hub nodes with Degree values greater than 2 times the median were screened as key critical components and key targets, respectively, and molecular docking was performed based on the key components obtained from the key target matching screening. The 3D structure of each component was downloaded using the PubChem website (https://pubchem.ncbi.nlm.nih.gov/), and the PDB structure of each target was downloaded using the PDB website (https://www.rcsb.org/). Each structure was hydrogenated and dehydrated in autodock software, and finally molecular docking was performed in AGFR software, and the molecular docking map was exported in PyMol software.

Animals

The Animal Care Committee of the Guangxi Institute of Chinese Medicine & Pharmaceutical Science approved the experiment, and all procedures of animal experiments were performed in accordance with the Laboratory Animal Management Regulations of China (1988, revised 2017). C57BL6j mice, male, weight 18–22 g, purchased from Changsha Tianqin Biotechnology Co., LTD. (Changsha, Hunan, China). All animals were fed on an SPF level laboratory with a 12 h daily/night cycle, a temperature of 25±1 °C and humidity of 60±10%.

Effects of AFPR on CORT-Induced Depression

C57BL/6j mice were randomly divided into control group, model group (CORT 20 $mg{\cdot}kg^{-1}$), positive group (CORT + fluoxetine 3.6 $mg{\cdot}kg^{-1}$), high-dose group (CORT + AFPR 40 $mg{\cdot}mL^{-1}$), middle-dose group (CORT + AFPR 20 $mg{\cdot}mL^{-1}$), and low-dose group (CORT + AFPR 10 $mg{\cdot}mL^{-1}$), 10 animals in each group. Except for the control group, mice in each group were injected intraperitoneally with CORT for 21 consecutive days for modeling, and then tested animal behavior. The positive drug and AFPR were administrated for 14 consecutive days, once a day, and behavioral testing was started on the 11th day of administration for 3 consecutive days.

Forced Swimming Test (FST)

A 20 cm×14 cm round glass tank was prepared, and 10 cm high water was added to the tank at a controlled temperature of (25±2)°C. The duration of swimming was 6 min for each mouse, starting from entering the water surface, the first 2 min were for acclimatization swimming, and the total time that the mice were floating on the water surface for the last 4 min was calculated.

Tail Suspension Test (TST)

The tail end of the mice was glued to the support of the hanging box (30 cm×30 cm×25 cm) with medical tape to make it hang upside down, with the head about 5 cm from the bottom of the box. A total of 6 min of tail hanging time was used for each mouse, the first 2 min was the adaptation time, and the total time of the mice hanging motionless in the last 4 min was calculated.

Cell Culture

Rat adrenal pheochromocytoma cells PC12 (Wuhan Pronosay Life Science and Technology Co., LTD.) were cultured in PC12 cells specific medium and stored in an incubator with 37°C temperature and 5% concentration of CO_2. PC12 cells were pretreated with CORT (200 $\mu mol{\cdot}L^{-1}$) for 24 h, then together treated with AFPR high-dose group (2 $mg{\cdot}mL^{-1}$), middle-dose group (1 $mg{\cdot}mL^{-1}$) and low-dose group (0.5 $mg{\cdot}mL^{-1}$) for 48 h.

Cytotoxicity Assays

The viability of PC12 cells was tested by CCK-8 assay. 1×10^4 cells per well were seeded into 96-well plate, and treated by AFPR for 24 h, then discarded the old medium, and added 100 μL of medium containing CCK-8 to each well (the ratio of CCK-8 to serum-free medium was 1:9), measured the OD value at 450 nm by Microplate Reader after 1 h of incubated in the incubator.

SiRNA and Cell Transfection

The sequence of siRNA targeting cAMP (si-cAMP) and negative control (NC) was purchased from RiboBio (Guangzhou, China). 1×10^6 cells per well were seeded into 6-well plate, transfection when the cells grow up to about 70%. Cells were divided into si-NC group, si-cAMP group, AFPR high-dose group (2 $mg\cdot mL^{-1}$), middle-dose group (1 $mg\cdot mL^{-1}$) and low-dose group (0.5 $mg\cdot mL^{-1}$). The si-NC group did not receive any treatment, while the other groups were treated with CORT (200 $\mu mol\cdot L^{-1}$) to induce depression model, then added si-cAMP reagent transfected for 24 h, and together treated with AFPR for 72 h.

ELISA

After the experiment, PC12 cell supernatants were collected and centrifuged, and mice were anesthetized with 2% sodium pentobarbital, then the blood was collected and centrifuged at 3000 rpm for 10 min, and the supernatant was taken and stored at −20 °C for backup. The levels of DA, 5-HT, NE, BDNF and β-NGF were measured according to the kit instructions.

H&E Staining

The specimens were fixed for 3 days in 4% paraformaldehyde fixative, paraffin embedded, cut into 5 μm slices, dewaxed in xylene, rehydrated in gradient ethanol, stained with hematoxylin, fractionated with 75% hydrochloric acid in alcohol, rinsed in water, stained with eosin, washed in water, dehydrated in gradient ethanol, transparent in xylene, dried and sealed with neutral resin.

Nissl Staining

Paraffin sections were sequentially placed in xylene I–xylene II–anhydrous ethanol I–anhydrous ethanol II–75% alcohol and then rinsed with water, stained with toluidine blue, washed with water, slightly differentiated with 0.1% glacial acetic acid, terminated with water, microscopic examination, washed with water. The slices were dried in an oven, transparent in xylene, and sealed with neutral resin. The brain tissue was dark blue in nisin and light blue in the background.

QRT-PCR

Total RNAs in PC12 cells were extracted with the TRIzol reagent and reversed transcription into cDNA with the PrimeScript RT Reagent Kit. QPRC was performed in a LightCycler 480 II Real-Time PCR thermocycler (Roche, Switzerland) with the ChamQ SYBR qPCR Master Mix. The primer of CREB and BDNF was synthesized by the biological company (Sangon, Shanghai, China). The forward sequences of CREB were 5'-TGGA GTTG TTAT GGCG TCCTC-3'; the reverse sequences of CREB were 5'-TCTC TTGC TGCT TCCC TGTTC-3'. The forward sequences of BDNF were 5'-CAGC GCGA ATGT GTTA GTGG TTA-3'; the reverse sequences of CREB were 5'-CAGT GGAC AGCC ACTT TGTT TCA-3'. The method of $2^{-\Delta\Delta CT}$ was used to calculate the relative expression of genes. GAPDH was used as the internal control gene.

Western Blot

Western blot were performed according to the literature[18], and the brief steps are as follows:

The total protein of mouse brain tissue (100 mg) and PC12 cells was extracted by adding 150 μL mixed lysate and BCA kit to quantify protein concentration. An equivalent denatured protein sample (100 μg) was added to each channel, separated by electrophoresis on a 12.5% sodium dodecyl sulfate-polyacrylamide gel, and transferred to a polyvinylidene difluoride membrane. The membrane was then closed with 5% skim milk powder solution at room temperature for 1

h and then incubated with the primary antibody overnight at 4°C. Antibody concentrations were PRKACA (1:1000), CREB (1:1000), p-CREB (1:1000), BDNF (1:1000), GAPDH (1:5000). The membranes were slowly washed 3 times with TRIS-buffered saline (TBST) on an oscillator for 5 minutes each. Then, the membranes were incubated with HRP-conjugated secondary antibody (1:5000) for 1 h at room temperature and finally washed 3 times with TBST. The gray values of each band were analyzed using Image J software.

Statistical Analysis

SPSS 22.0 (SPSS, Inc., Chicago, IL, USA) was used to analyze the data as mean±SD, and the data of each group were first tested for normal distribution and chi-square test, and if they were normally distributed and chi-square, one-way ANOVA was used to compare the groups. $P<0.05$ indicated that the results were significant. GraphPad Prism 8.0 was used for graphing.

Results

Compounds Analysis of AFPR

The chemical compounds of AFPR were predicted by GC-MS analysis, as shown in Figure 1, a total of 8 compounds were analyzed in AFPR, namely, tetradecanoanoic acid, methyl ester; hexadecenoic acid, methyl ester; hexadecanoic acid, methyl ester; 14-methyl-pentadecanoic acid, methyl ester; Octadecadienoic acid, methyl ester; e-Octadecenoic acid, methyl ester; z-Octadecenoic acid, methyl ester and heptadecanoic acid, methyl ester, as listed in Table 1.

The Collection of Drug Compound Targets and Depression Targets

A total of 306 drug compound targets were obtained from the Swiss Target Prediction database and the TCMIP database. Furthermore, a total of 545 depression targets were obtained after combining the prediction results from five databases.

Potential Targets of AFPR on Antidepressant

A total of 52 joint targets were obtained after compared 306 drug compound targets and 545 depression targets by online Venn diagram. As shown in Figure 2A, the joint targets are the potential targets of AFPR for depression. As shown in Figure B, the 52 joint targets were plotted in a PPI network using the STRING website. We then visualized the PPI network file by Cytoscape software and analyzed its network feature values, and the median was calculated to be 3 according to the Degree value. A total of 4 Hub nodes were obtained after screening, namely PTPN11, ESR1, NR3C1, MAPK1, as shown in Figure 2C, key targets were located in the inner cycle, the other targets were located in the outer cycle, and the color changes with the Degree value, the darker the color indicates the larger the Degree value. The "drug-target-disease" network diagram of AFPR antidepressant was constructed using Cytoscape software, as shown in Figure 2D, the blue oval represents the drug compounds, the green square represents the remaining targets, and the orange triangle represents the key targets.

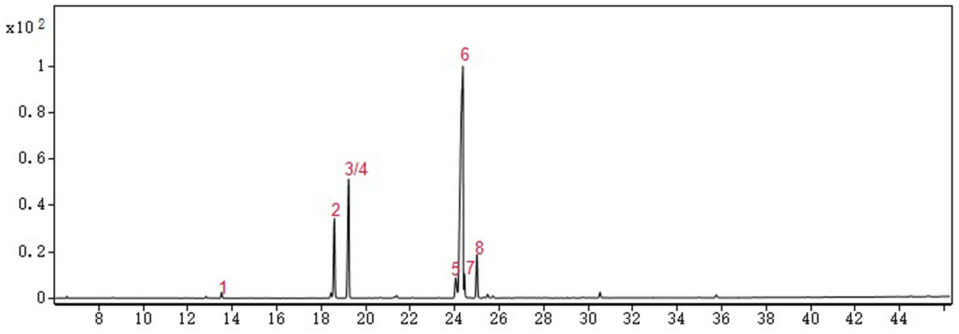

Figure 1 GC-MS diagram of AFPR acidic methylation.

Table 1 Identification of AFPR Acid Methyl Esters by GC-MS

Peak No.	Rt/min	Compound Name	Formula
1	13.52	Tetradecanoanoic acid, methyl ester	$C_{15}H_{30}O_2$
2	18.59	Hexadecenoic acid, methyl ester	$C_{17}H_{32}O_2$
3	19.23	Hexadecanoic acid, methyl ester	$C_{17}H_{34}O_2$
4	19.24	14-methyl-pentadecanoic acid, methyl ester	$C_{17}H_{34}O_2$
5	24.06	Octadecadienonic acid, methyl ester	$C_{19}H_{34}O_2$
6	24.22	E-Octadecenoic acid, methyl ester	$C_{19}H_{36}O_2$
7	24.37	Z-Octadecenoic acid, methyl ester	$C_{19}H_{36}O_2$
8	25.00	Heptadecanoic acid, methyl ester	$C_{19}H_{38}O_2$

GO and KEGG Signaling Pathway Analysis of AFPR on Antidepressant

The 52 potential targets were analyzed using the DAVID database, and 269 GO entries were obtained, including 167 biological process (BP), 49 cell composition (CC), and 53 molecular function (MF). The top 10 entries for each of BP, CC and MF entries were selected based on the *P*-values to draw the diagram using the Microbiology website, as shown in

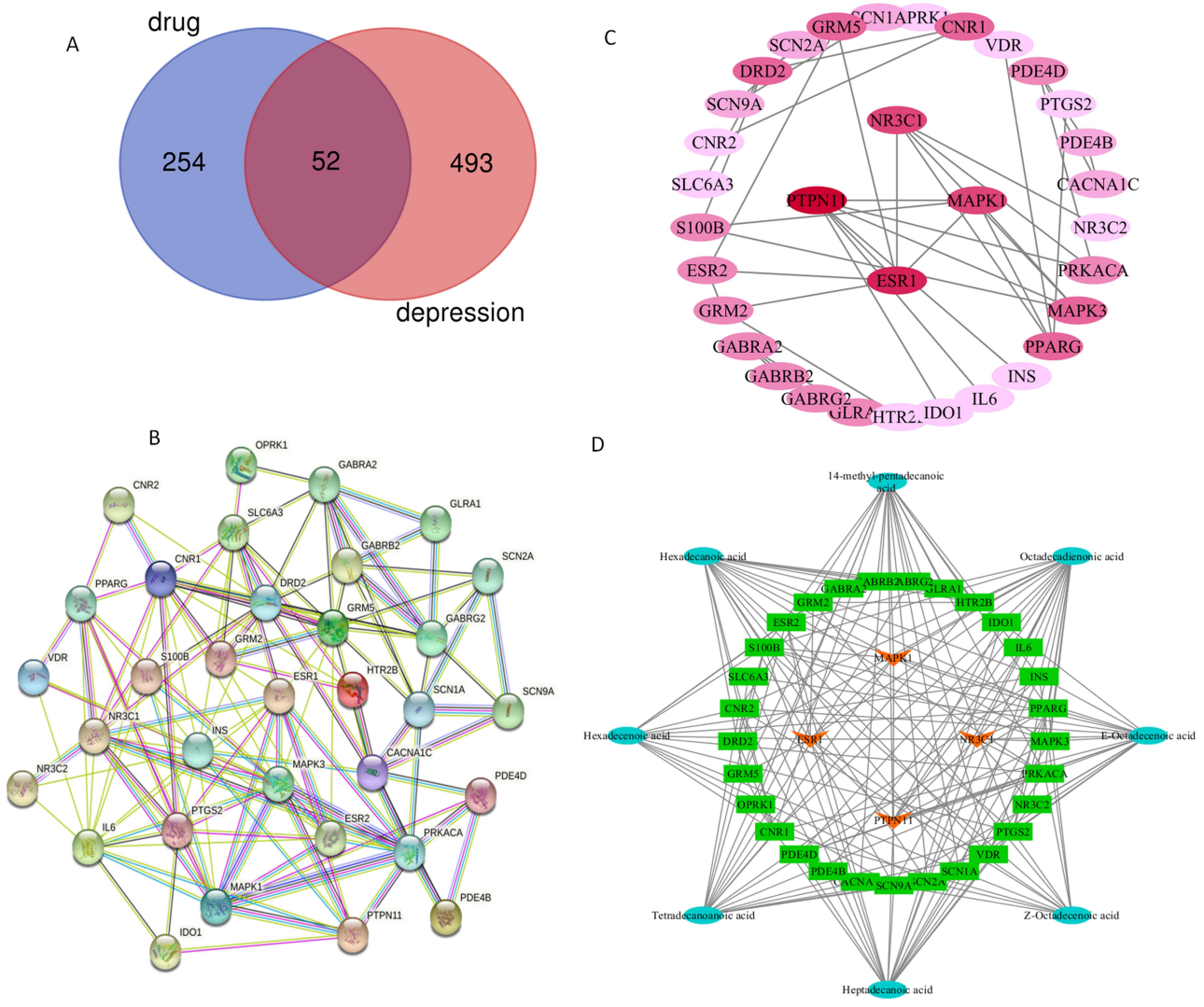

Figure 2 Potential targets of AFPR on antidepressant. (**A**) Venn diagram; (**B**) PPI network diagram; (**C**) Key targets and other targets of AFPR on depression; (**D**) "Drug-target- Disease" network diagram.

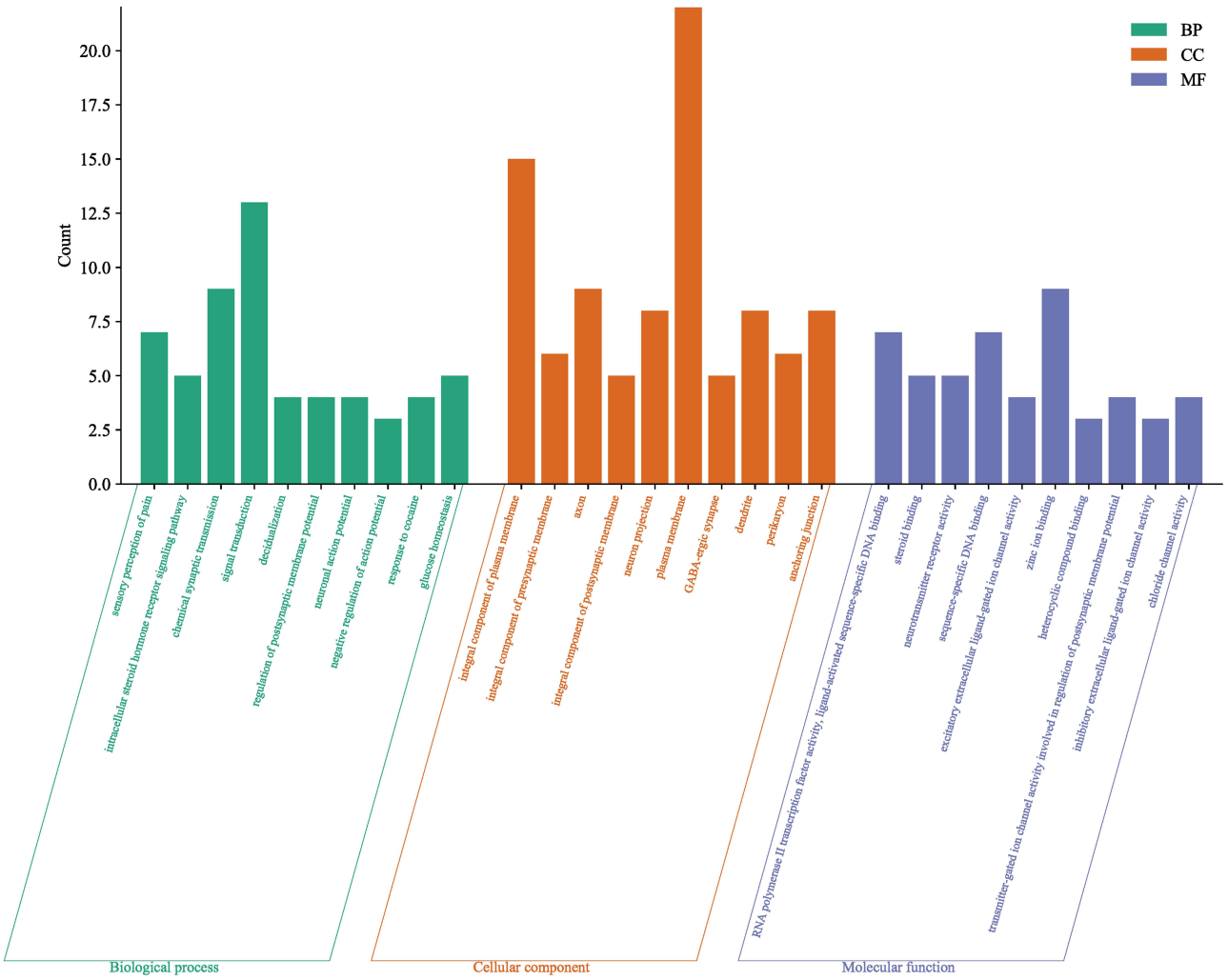

Figure 3 GO analysis diagram.

Figure 3. BP mainly includes intracellular steroid hormone receptor signaling pathway, chemical synaptic transmission, signal transduction, regulation of postsynaptic membrane potential, neuronal action potential, etc.; CC mainly includes integral component of presynaptic membrane, integral component of postsynaptic membrane, dendrites, neuronal projections, etc.; MF mainly includes RNA polymerase II transcription factor activity, ligand-activated sequence-specific DNA binding, steroid binding, neurotransmitter receptor activity, excitatory extracellular ligand-gated ion channel activity, zinc ion binding, etc.

The 52 potential targets were analyzed using the DAVID database, and 84 KEGG pathways were obtained. The top 20 were selected to draw bubble diagrams using the microbiology website, as shown in Figure 4. The results showed that the main signaling pathways of AFPR on anti-depression mainly included cAMP signaling pathway, phospholipase D signaling pathway, and C-type lectin receptor signaling pathway.

Molecular Docking

Based on the Degree values more than 2 times of the median, a total of 4 chemical compounds were selected to be key compounds, namely octadecadienoic acid (OCT), hexadecenoic acid (HEXE), hexadecanoic acid (HEXA) and 14-methyl-pentadecanoic acid (14-MET); and a total of 2 Hub notes were selected to be key targets using the same method, namely ESR1 and MAPK1. Selecting corresponding key chemical compounds based on the 2 key targets and 5 groups of key compound-target proteins were obtained, namely, OCT-MAPK1, OCT-ESR1, HEXE-ESR1, HESA-MAPK1 and 14-MET-MAPK1. The

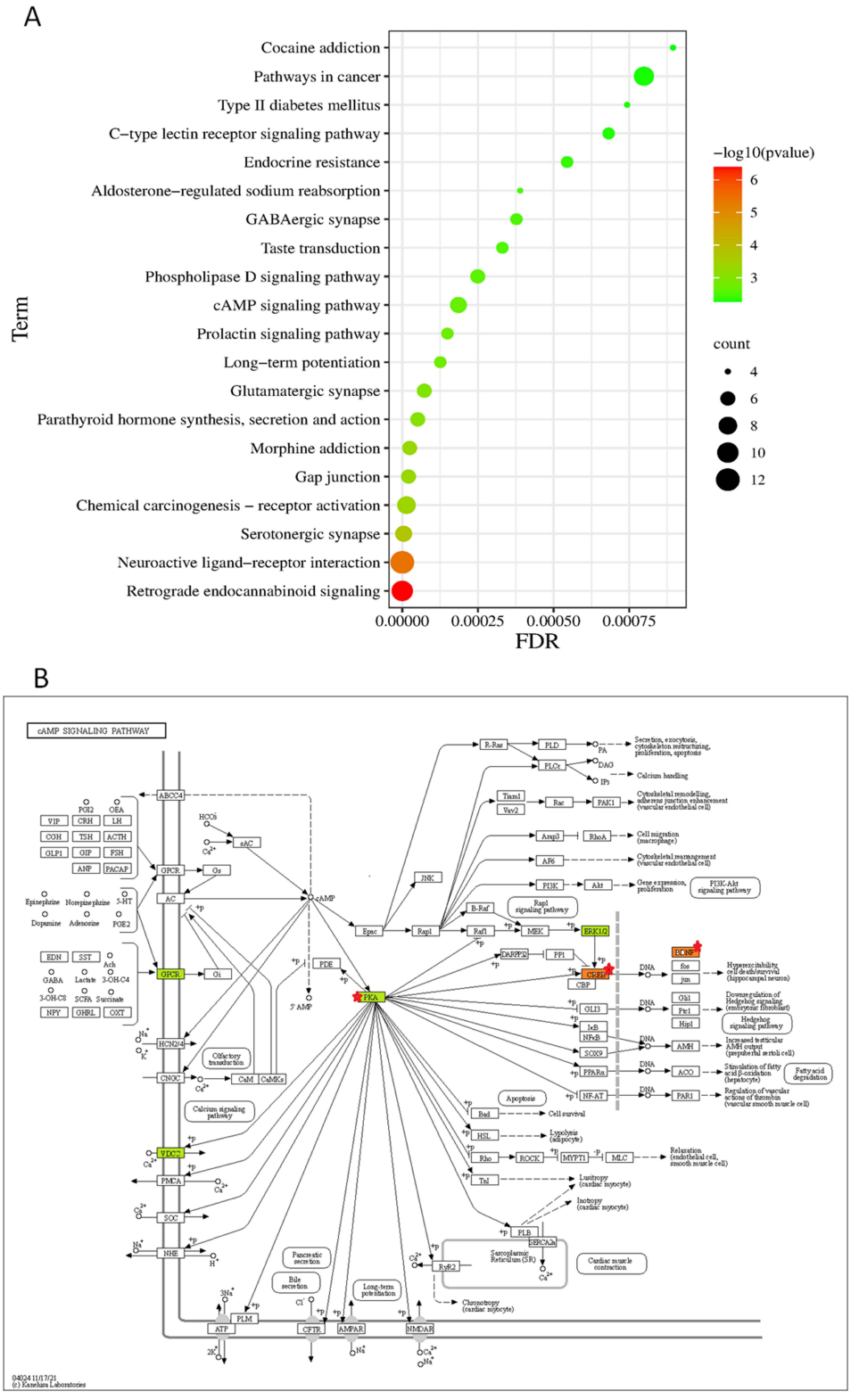

Figure 4 KEGG signaling pathway diagram.

Notes: A: KEGG signaling pathway. The change in pvalue from red to green indicates the level of significance, with the redder the color, the higher the significance. Conversely, greener indicates lower significance. The higher the number of counts, the larger the circle, and vice versa, the smaller the circle. B: cAMP signaling pathway. The asterisk indicate genes related to neuroplasticity.

Table 2 The Results of Molecular Docking

Compound	Target	Energy (kJ/mol)
Octadecadienonic acid	MAPK1	−17.1544
Octadecadienonic acid	ESR1	−13.8072
Hexadecenoic acid	ESR1	−21.3384
Hexadecanoic acid	MAPK1	−16.3176
14-methyl-pentadecanoic acid	MAPK1	−19.2464

molecular docking results are shown in Table 2 and Figure 5, among them, the smallest binding energy was HEXE-ESR1, indicating that they have a stable binding ability.

Effects of AFPR on CORT-Induced Behavior in Mice

The forced swimming test (FST) and the tail suspension test (TST) are classic experiments in depression. As shown in the Figure 6A and B, after 21 days of modeling with CORT, the immobility time of FST ($P < 0.01$) and TST ($P < 0.01$ or

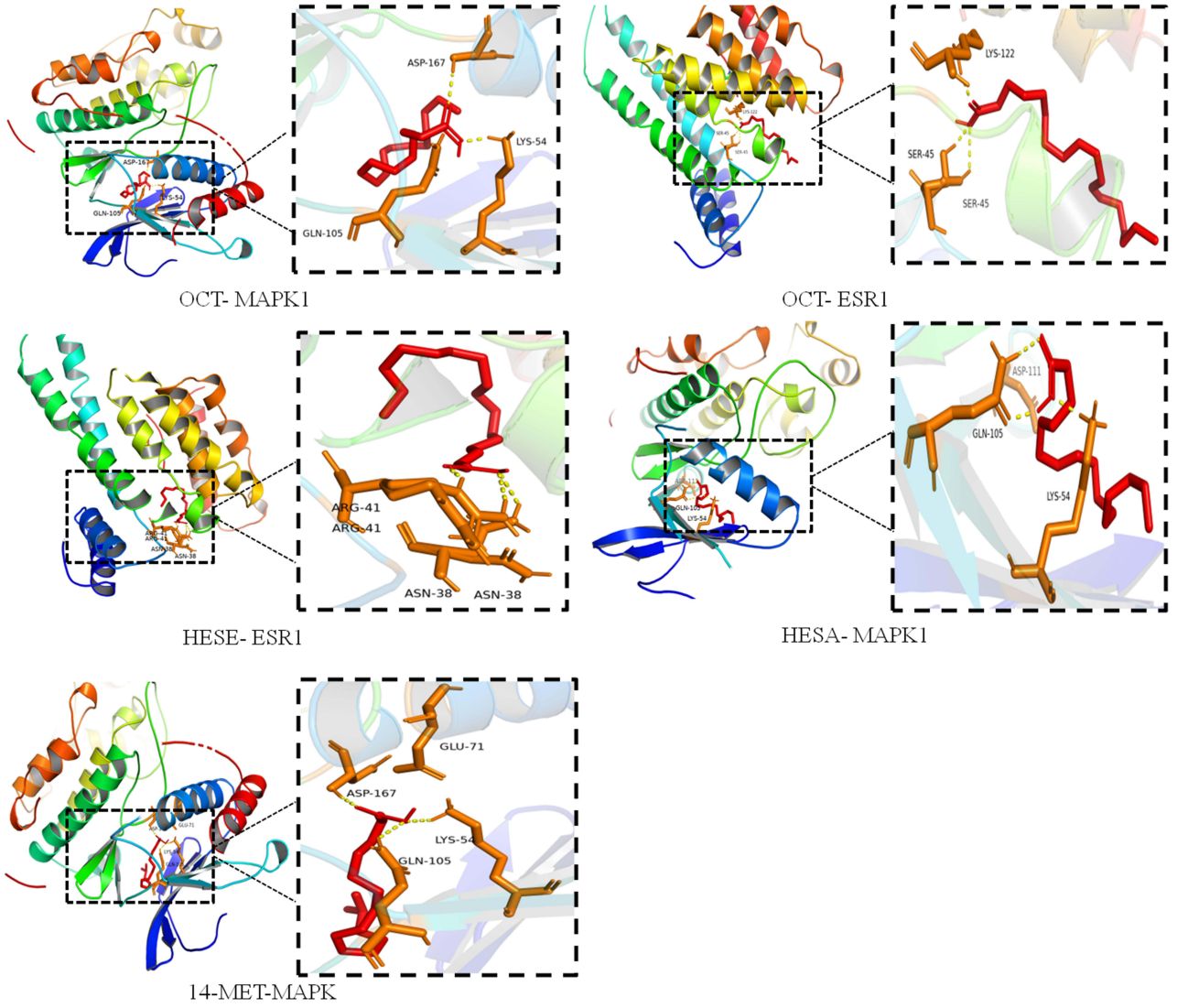

Figure 5 Results of molecular docking.

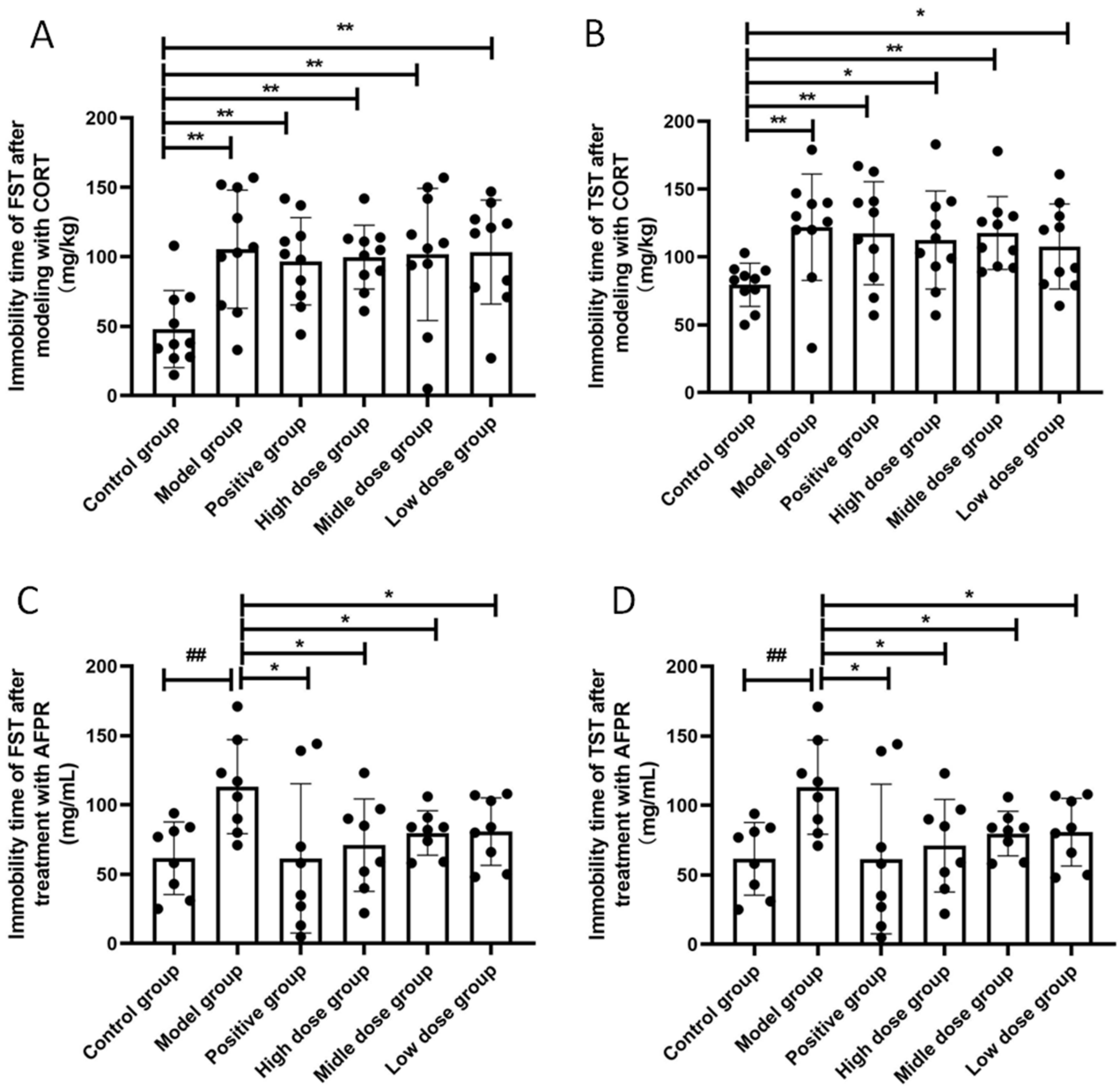

Figure 6 Effects of AFPR on behavior in mice. (**A**) Immobility time of FST after modeling with CORT. (**B**) Immobility time of TST after modeling with CORT. (**C**) Immobility time of FST after treatment with AFPR. (**D**) Immobility time of TST after treatment with AFPR. Data are represented as the mean ± SD (n=10 or n=8). $^{\#\#}P< 0.01$ compared to the control group, $^{*}P< 0.05$, $^{**}P< 0.01$ compared to the model group.

$P < 0.05$) in the rest of groups were significantly increased compared to the control group, indicating that CORT successfully induced depression. However, after treatment with AFPR, the immobility time of FST ($P < 0.05$) and TST ($P < 0.05$) were significantly decreased compared to the model group (Figure 6C and D), indicating that AFPR has an ameliorate effect on depressive behavior.

Effect of AFPR on the Serum of CORT-Induced Depression Mice

To observe the effect of AFPR on CORT-induced depression, the levels of 5-HT, DA, NE, BDNF, β-NGF and NF-κB were measured by ELISA. The result (Figure 7) was shown that compared with control group, the levels of 5-HT, DA, NE, BDNF and β-NGF in the model group were significantly decreased ($P < 0.01$, $P < 0.05$, $P < 0.05$, $P < 0.01$, $P < 0.05$), and the level of NF-κB in the model group was significantly increased ($P < 0.01$), indicating that CORT

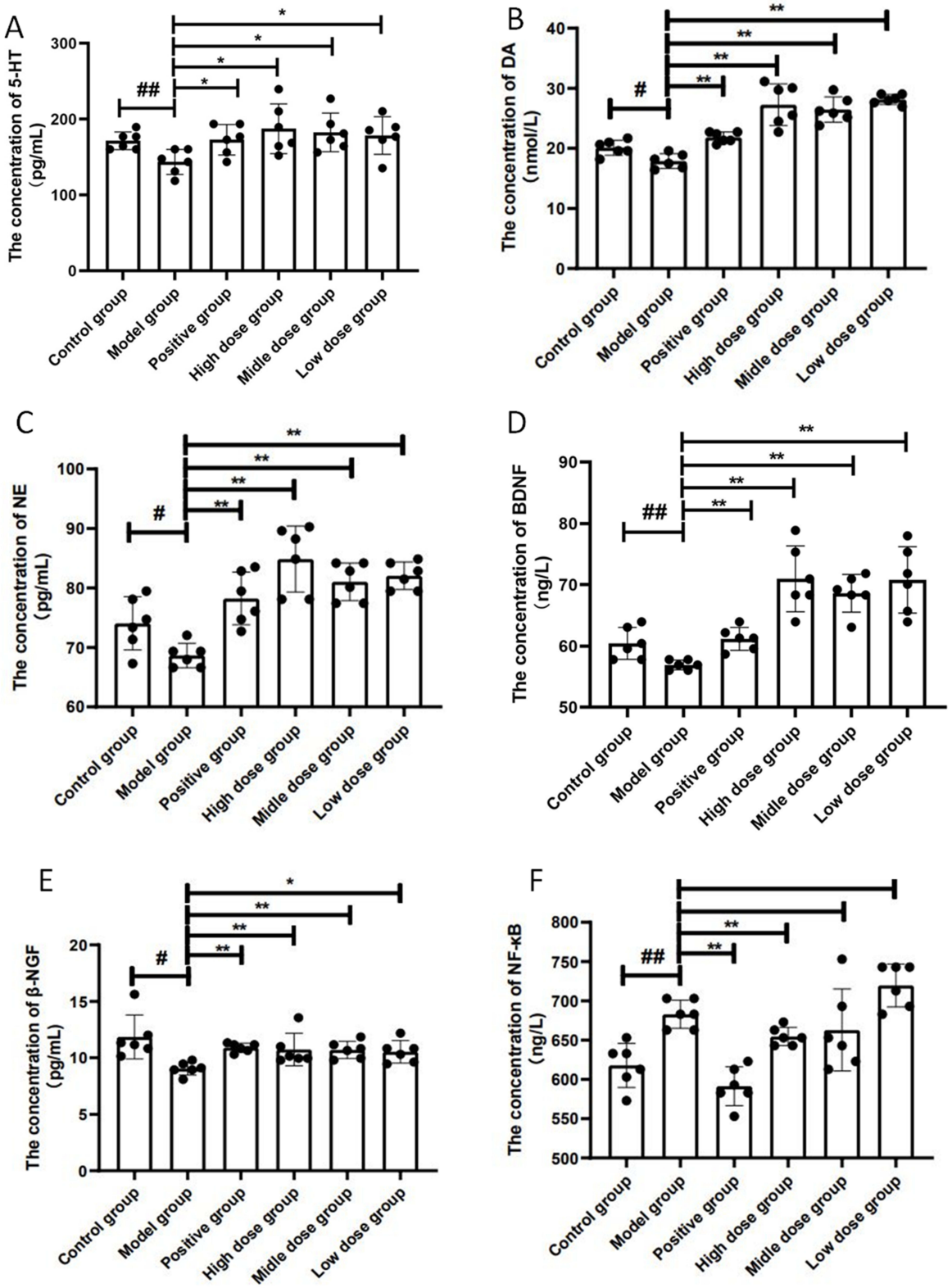

Figure 7 Effect of AFPR on the serum of CORT-induced depression mice. (**A**) The concentration of 5-HT. (**B**) The concentration of DA. (**C**) The concentration of NE. (**D**) The concentration of BDNF. (**E**) The concentration of β-NGF. (**F**) The concentration of NF-κB. Data are represented as the mean ± SD (n=6). $^{\#}P< 0.05$, $^{\#\#}P< 0.01$ compared to the control group, $^{*}P< 0.05$, $^{**}P< 0.01$ compared to the model group.

successfully induce depression. While treatment with AFPR, compared with model group, the levels of 5-HT, DA, NE, BDNF and β-NGF in the high-dose group were significantly increased ($P < 0.05$, $P < 0.01$, $P < 0.01$, $P < 0.01$, $P < 0.01$), and the level of NF-κB in the high-dose group was significantly decreased ($P < 0.01$). The levels of 5-HT, DA, NE, BDNF and β-NGF in the middle- and low-dose groups showed the same trend with the high-dose group; however, the level of NF-κB in those two groups did not show any statistical significance. These data showed that AFPR improved neurotransmitter and alleviated inflammation in the serum of depression mice.

Effect of AFPR on Neuron Cells in Mice

To further observe the effects of AFPR on prefrontal cortex and hippocampal neurons, H&E and Nissl staining were performed. As shown in Figure 8a–f, compared with the control group, the prefrontal cortex neuronal cells were damaged in the model, which showed nucleus fixation, cell necrosis and increased glial cell differentiation. However, compared with the model group, the drug administration group significantly improved the above pathological changes. As shown in Figure 8g–l, the hippocampal neurons in the model group were damaged, as shown by the decrease of Nissl vesicles and lighter color; while compared with the model group, the above phenomenon was improved in the drug administration group. These data indicated that AFPR ameliorated damage to prefrontal cortex and hippocampal neurons in depressed mice.

Effect of AFPR on cAMP Signaling Pathway in the Brain of Depressive Mice

The above network pharmacology predicts that the antidepressant effect of AFPR may be related to cAMP signaling pathway. Western blot was used to verify this result. As shown in Figure 9, compared with control group, the expression of BDNF, p-CREB and PRKACA was significantly decreased in the model group ($P < 0.05$, $P < 0.05$, $P < 0.05$). However, the expression of BDNF, p-CREB and PRKACA was significantly increased after treating with AFPR, except that the expression of p-CREB/CREB in the low-dose group. These results demonstrated that AFPR ameliorated depression through cAMP signaling pathway, which was corresponding with the predicted result.

Effect of AFPR on CORT-Induced PC12 Cells

Next, we investigated the effect of AFPR on depression in vitro. First, the toxic effects of different concentrations of AFPR on cells were determined by three parallel experiments using the CCK-8 method, and the results showed that the IC50 obtained in the first panel was 4.008 $mg \cdot kg^{-1}$, the IC50 obtained in the second panel was 3.892 $mg \cdot kg^{-1}$, and the IC50 obtained in the third panel was 4.092 $mg \cdot kg^{-1}$, indicating that the AFPR on PC12 cells IC50 was about 4 $mg \cdot kg^{-1}$.

Then, the expression of neurotransmitters and neurotrophic factors in PC12 cell supernatants was measured by ELISA and the results (Figure 10A–D) showed that, compared to control group, the expression of 5-HT, DA and BDNF was significantly decreased ($P < 0.05$, $P < 0.01$, $P < 0.01$) and the expression of MAO was significantly increased ($P < 0.01$) in the model group. While treated with AFPR, the expression of 5-HT, DA, MAO and BDNF was significantly reversed. These data showed that AFPR improved neurotransmitter and neurotrophic factors in the supernatants of CORT-induced PC12 cells.

Last, the key targets of the cAMP signaling pathway—CREB and BDNF—were detected by qRT-PCR. As shown in Figure 10E and F, compared to control group, the expression of CREB and BDNF in model group were significantly decreased ($P < 0.01$, $P < 0.01$), and this condition was reversed by AFPR treatment. These results demonstrated that AFPR may improve neuroplasticity via the cAMP signaling pathway to improve depression-like symptoms in vitro.

AFPR Improved Depression Through cAMP Signaling Pathway

To further investigate the effect of cAMP signaling pathway on depression and whether AFPR ameliorate depression by regulating downstream targets through cAMP, we interfered with the cAMP gene. The results of western-blot (Figure 11B–D) were showed that the expression of BDNF, p-CREB and PRKACA in the si-cAMP group was significantly decreased ($P < 0.01$, $P < 0.01$, $P < 0.05$), indicating that cAMP is a key target affected the progress of

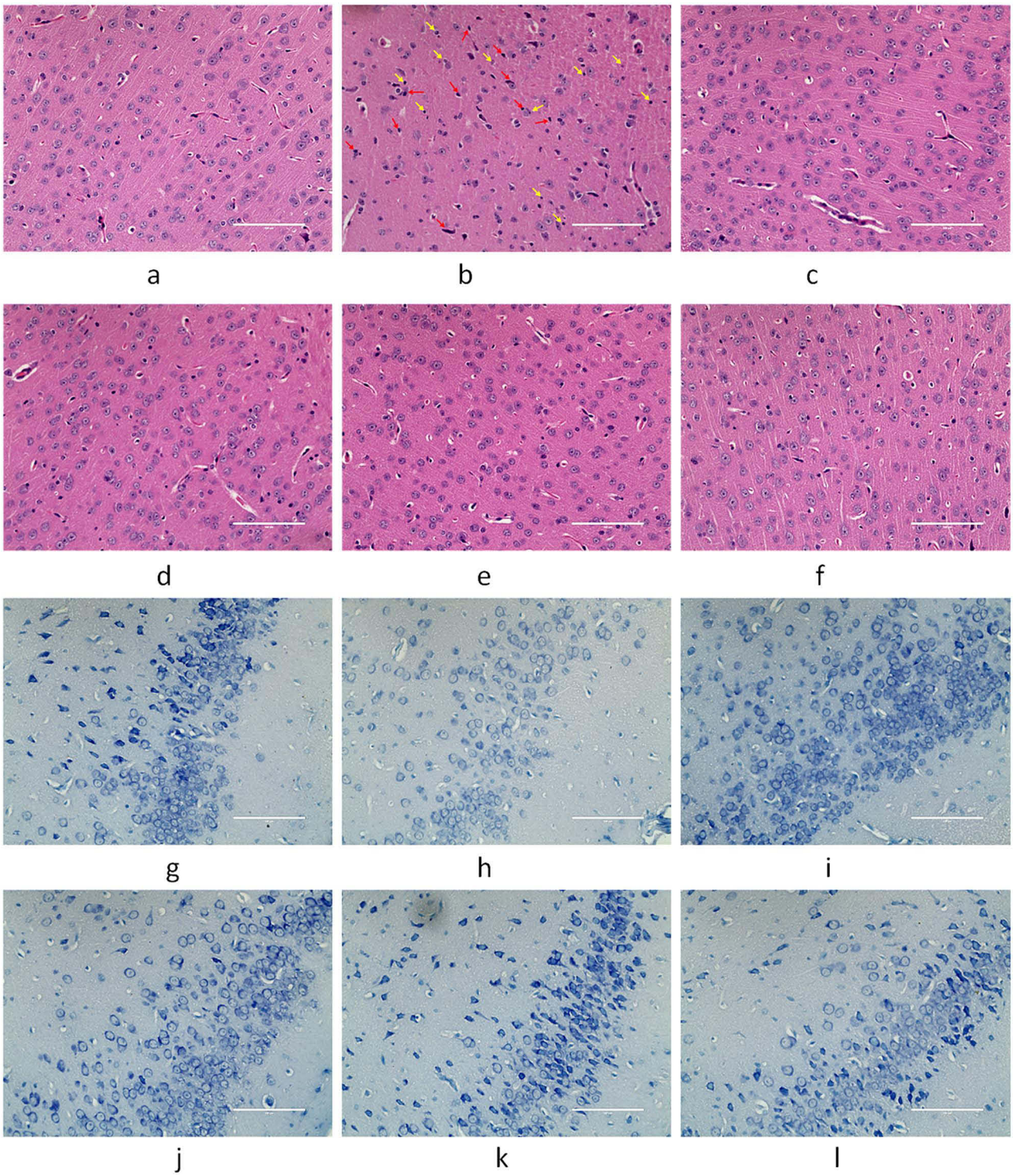

Figure 8 Effect of AFPR on neuron cells. (**a**–**f**) H&E staining (40×). (**g**–**l**) Nissl staining (40×). (**a** and **g**) Control group; (**b** and **h**): model group; (**c** and **i**) positive group; (**d** and **j**) high dose group; (**e** and **k**) middle dose group; (**f** and **l**) low dose group. In (**b**), red arrows indicate glial cells; yellow arrows indicate nuclear fixation and necrosis.

depression. However, the expression of p-CREB, BDNF and PRKACA was significantly increased after treating with high dose of AFPR ($P < 0.05$, $P < 0.05$, $P < 0.05$).

Finally, to observe whether cAMP deficiency causes functional changes in depression, ELISA was used to detect the levels of neurotransmitters and neurotrophic factors in the supernatants of PC12 cells. As shown in Figure 11E–G,

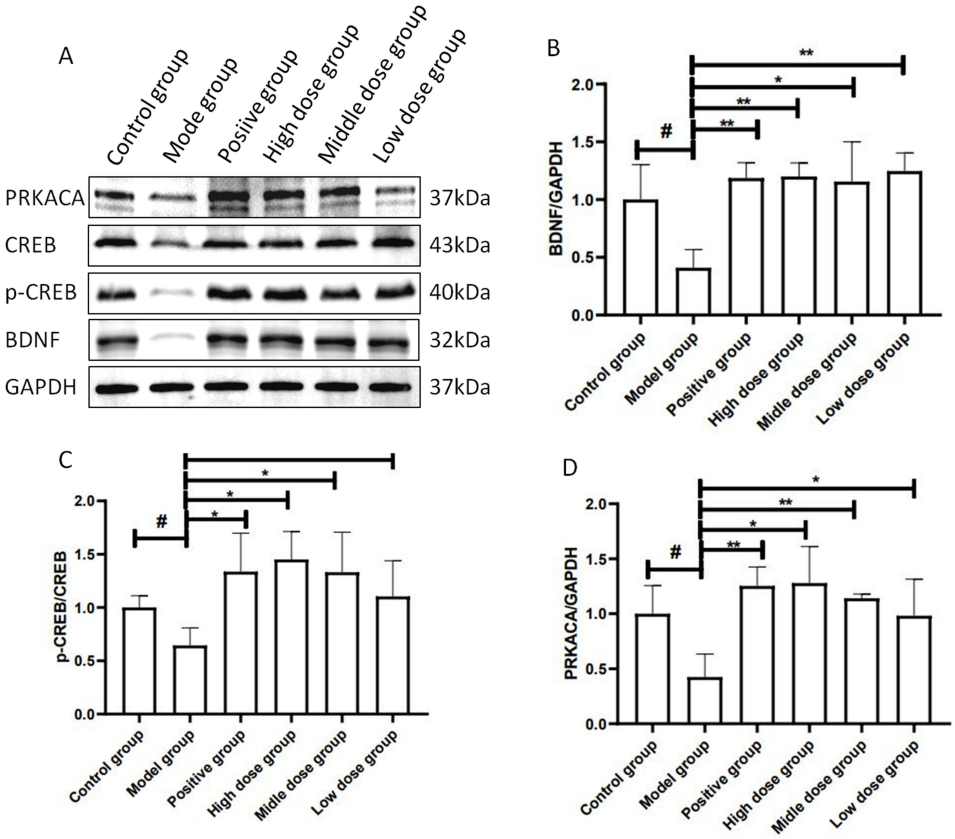

Figure 9 Effect of AFPR on cAMP signaling pathway. (**A**) Western Blot strips. (**B**) BDNF/GAPDH. (**C**) p-CREB/CREB. (**D**) PRKACA/GAPDH. Data are represented as the mean ± SD (n=3). $^{\#}P< 0.05$ compared to the control group, $^{*}P< 0.05$, $^{**}P< 0.01$ compared to the model group.

compared with si-NC group, the expression of 5-HT, BDNF and NE in the si-cAMP group was significantly decreased ($P < 0.01$, $P < 0.01$, $P < 0.05$), indicating that cAMP deficiency affects the function of depression. However, compared with si-cAMP group, the expression of 5-HT, BDNF and NE was significantly reversed by treatment of high dose of AFPR. These data revealed that AFPR could ameliorate depression via cAMP signaling pathway.

Discussion

Studies have shown that depression models include chronic mild stress model, inescapable stress and social failure stress model, etc., but no matter which model, it will eventually activate the HPA axis, leading to the secretion of CORT. Therefore, long-term systemic administration of CORT was used as an additional model of depression.[18,19] It was reported that CORT-treated animals exhibit several behavioral features similar to depression, including enhanced behavioral despair in the FST and anhedonia in the sucrose preference test (SPT).[20–22] In this study, we found that AFPR significantly shortened the immobility time of FST and TST in mice and increased the levels of neurotransmitters, neurotrophic factors and nerve growth factors in serum, which showed significant effects on improving depression. However, the pathogenesis of depression is complex. Studies have shown that abnormal excitatory synapses,[23] over-activated microglia,[24] neuroimmunity, neuroinflammation,[25] and neuronal autophagy[26] are all related to the attack of depression. New studies have shown that at the molecular level, depression is characterized by neuroplastic dysfunction, including medial prefrontal cortex and hippocampal neuronal atrophy and synaptic inhibition.[27] In our study, the pathological results showed that AFPR ameliorated the atrophy of prefrontal cortex and hippocampal neurons, suggesting that AFPR may improve depression-like symptoms by improving neuroplasticity function.

The specific antidepressant mechanism of action of AFPR still remains to be elucidated, and the emergence of network pharmacology has undoubtedly provided important ideas for the study of the mechanism of depression treatment

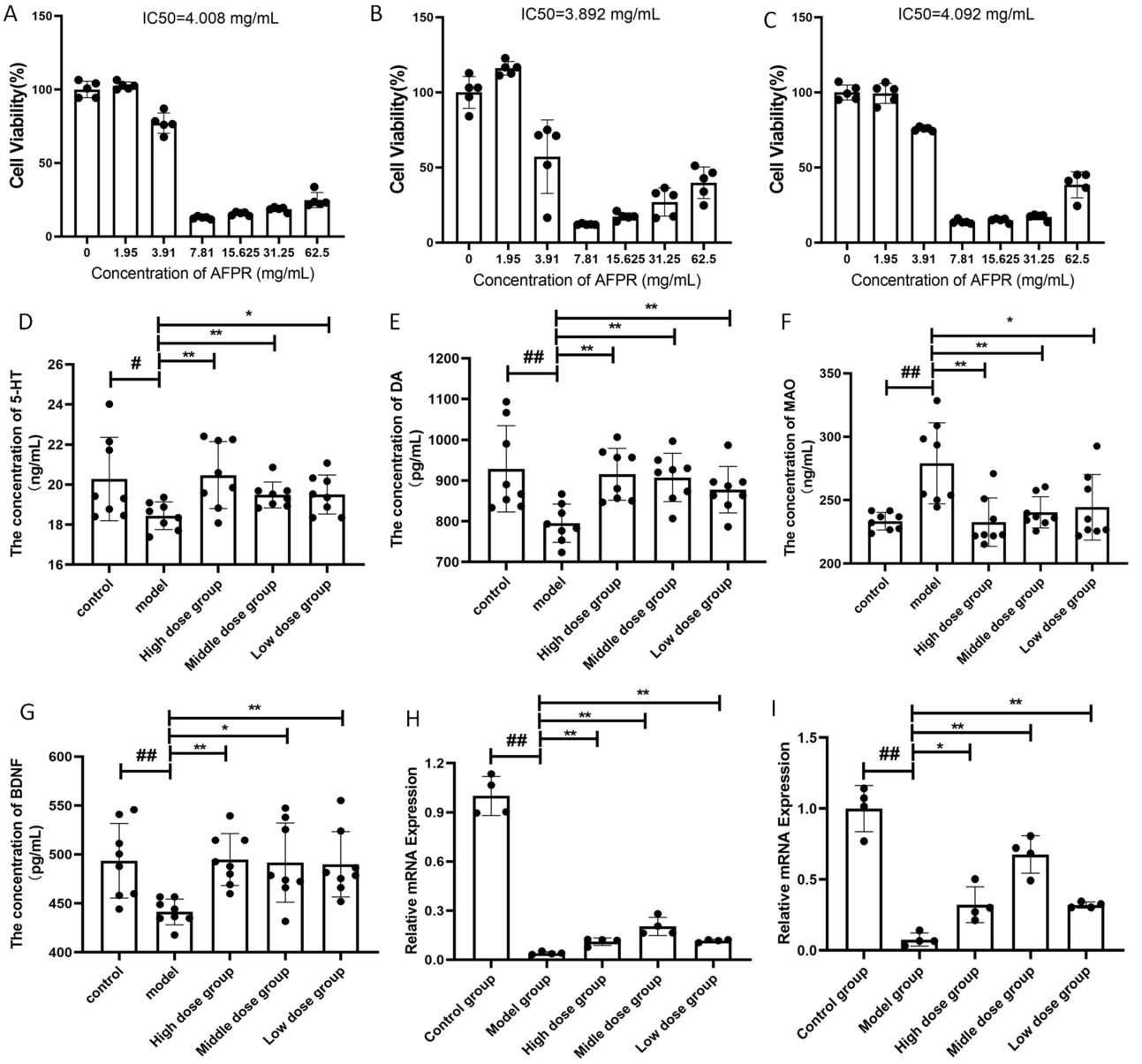

Figure 10 Effect of AFPR on CORT-induced PC12 cells. (**A**–**C**): Cell viability (%). (**D**) The concentration of 5-HT. (**E**) The concentration of DA. (**F**) The concentration of MAO. (**G**) The concentration of BDNF. (**H**) Relative mRNA expression of CREB. (**I**) Relative mRNA expression of BDNF. Data are represented as the mean ± SD (n=5, n=8 or n=4). $^{\#}P< 0.05$, $^{\#\#}P< 0.01$ compared to the control group, $^{*}P< 0.05$, $^{**}P< 0.01$ compared to the model group.

by herbal medicine. In this study, we conducted in-depth information mining of AFPR through network pharmacology. Based on the analysis results of network pharmacology, we obtained a total of 306 targets, 8 active ingredients and 52 potential antidepressant targets for AFPR and included a total of 4 core targets. The results of GO analysis showed that most of the important processes of antidepressant of AFPR were related to chemical synaptic transmission, neuronal action potential, etc. The results of KEGG enrichment analysis showed that the antidepressant processes of AFPR were mainly related to cAMP signaling pathway, phospholipase D signaling pathway, C-type lectin receptor signaling pathway, etc. The molecular docking results showed that the key components and key targets obtained from the screening had binding ability, and among them, the hexadecanoic acid and ESR1 protein binding the most stable. The above results suggest that AFPR may exert antidepressant effects through multiple components, multiple targets and multiple pathways. Furthermore, the cAMP signaling pathway is related to neuroplasticity in depression. Based on the results of the previous study and the predicted results of network pharmacology, we further investigated the cAMP pathway and

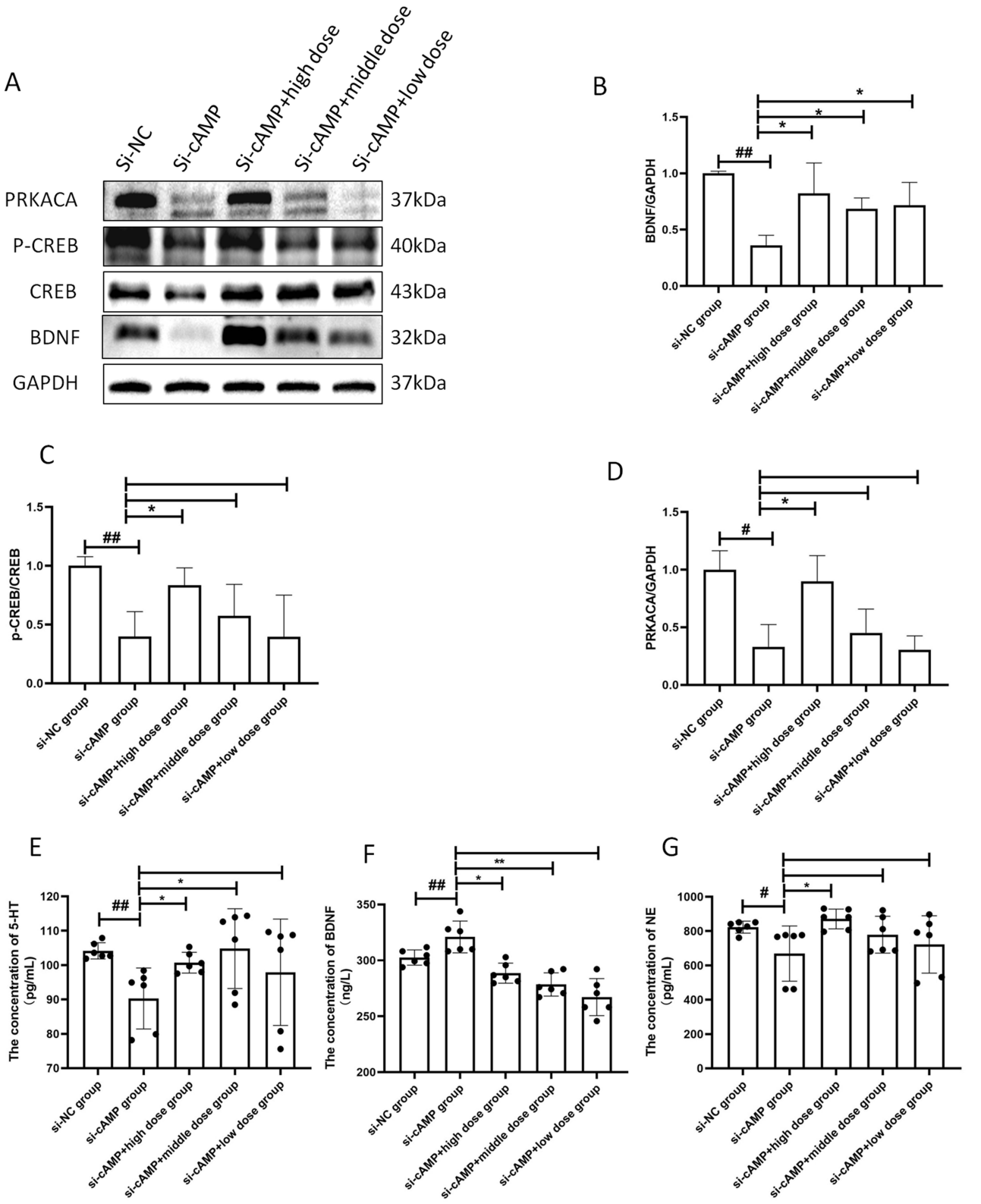

Figure 11 AFPR improved depression through cAMP signaling pathway. (**A**) Western Blot strips after interference of cAMP. (**B**) BDNF/GAPDH. (**C**) p-CREB/CREB. (**D**) PRKACA/GAPDH. (**E**) The concentration of 5-HT. (**F**) The concentration of BDNF. (**G**) The concentration of NE. Data are represented as the mean ± SD (n=3 or n=6). $^{\#}P< 0.05$, $^{\#\#}P< 0.01$ compared to the control group, $^{*}P< 0.05$, $^{**}P< 0.01$ compared to the model group.

showed that AFPR significantly increased the expression of key proteins PRKACA, CREB, and BDNF in the cAMP pathway, indicating that AFPR may improve depression-like symptoms by regulating the cAMP pathway.

Studies showed that cAMP/PKA/CREB signaling pathway is closely related to glutamatergic synaptic plasticity.[28,29] As an important second messenger, cAMP can participate in the process of learning and memory and the changes of long-term synaptic plasticity. It can also activate cAMP-dependent protein kinase a (PKA), which can phosphorylate cAMP response element protein (CREB).[30] CREB is a transcription factor, and unphosphorylated CREB is located mainly in the nucleus. CAMP activates PKA, which enters the nucleus and activates CREB through phosphorylation of the amino-terminal kinase-inducible domain (KID), thereby regulating the transcription of target genes. BDNF is the target gene of CREB and is a neurotrophic factor widely expressed in the nervous system that promotes neuronal survival and differentiation and induces neurosynaptic growth during brain development.[31–33] Studies have shown that CREB family transcription factors are the main regulators of BDNF gene expression after TrkB signaling. The CREB transcription factor family regulates BDNF transcription, especially the activation of BDNF promoter IV and promoter I in response to neuronal activity.[34] Unlike CREB, PRKACA is a cAMP-dependent protein kinase. In depression, PRKACA activation by cAMP drives CREB phosphorylation, which causes downstream changes.

SiRNA is a class of synthetic double-stranded RNA – consisting of a righteous strand and an antisense strand, usually 21 nt in length. The antisense strand exerts its post-transcriptional regulatory function by pairing with mRNA in a fully complementary manner, thereby degrading the mRNA. In the present study, synthetic si-cAMP entered the cells through cytocytosis and eventually caused downstream mRNA degradation, while treatment by AFPR significantly increased the levels of 5-HT, NE and BDNF in the cell supernatant; decreased the levels of MAO in the cell supernatant; and increased the expression of PRKACA, CREB and BDNF proteins in PC12 cells, suggesting that AFPR can improve neuroplasticity via the cAMP signaling pathway to improve depression-like symptoms.

Conclusion

In summary, the network pharmacology results suggest that AFPR exert antidepressant effects through multiple components, targets and pathways. The experimental validation results showed that AFPR significantly increase the levels of neurotransmitters and neurotrophic factors, increase the expression of key proteins in the cAMP signaling pathway, and improve the atrophy of prefrontal cortex and hippocampal neurons. The above results suggest that AFPR could improve depression-like symptoms via cAMP signaling pathway. However, how AFPR regulates the cAMP pathway remains to be elucidated. Our next experiments will continue to explore how AFPR acts on cAMP pathway to improve depression, with the aim of providing an experimental basis for developing AFPR as a new antidepressant.

Funding

This research was funded in part by National Natural Science Foundation of China (81960729, 82260776, 81960164), Guangxi Traditional Chinese Medicine Key Discipline Construction Project (GZXK-Z-20-75), Science and Technology Major Project of Guangxi (AB21196020).

Disclosure

The authors report no conflicts of interest in this work.

References

1. Berger S, Gureczny S, Reisinger SN, Horvath O, Pollak DD. Effect of chronic corticosterone treatment on depression-like behavior and sociability in female and male C57bl/6n mice. *Cells*. 2019;8:1018. doi:10.3390/cells8091018
2. Kessler RC, Berglund P, Demler O, et al.; National Comorbidity Survey, R. The epidemiology of major depressive disorder: results from the National Comorbidity Survey Replication (Ncs-R). *JAMA*. 2003;289:3095–3105. doi:10.1001/jama.289.23.3095
3. Bansal Y, Kuhad A. Mitochondrial dysfunction in depression. *Curr Neuropharmacol*. 2016;14:610–618. doi:10.2174/1570159X14666160229114755
4. Lang UE, Borgwardt S. Molecular mechanisms of depression: perspectives on new treatment strategies. *Cell Physiol Biochem*. 2013;31:761–777. doi:10.1159/000350094
5. Lin Y, Yang W, Cao N, Zhao L. Comparison on antidepressant effects of modified xiaoyao powder. *Chin Herb Med*. 2021;52:137–144 doi:10.7501/j.issn.0253-2670.2021.01.017.

6. Sharma R, Singla RK, Banerjee S, Sinha B, Shen B, Sharma R. Role of Shankhpushpi (Convolvulus pluricaulis) in neurological disorders: an umbrella review covering evidence from ethnopharmacology to clinical studies. *Neurosci Biobehav Rev*. 2022;140:104795. doi:10.1016/j.neubiorev.2022.104795
7. He J, Zhu F, Li D, Wei J, Fan J, Wei G. Effect of Mahonia bealei Leaf Extract on Inflammation in Depression of Rats via NF-KB/NLRP3 Signaling Pathway. *Chin J Exper Formul*. 2022;28:67–74 doi:10.13422/j.cnki.syfjx.202201005.
8. Huang X, Wei J, Lu M. Guangxi standard of traditional Chinese medicinal materials (volume Ii); 1996, 255–258.
9. Chen Y, Kern TS, Kiser PD, Palczewski K. Eyes on systems pharmacology. *Pharmacol Res*. 2016;114:39–41. doi:10.1016/j.phrs.2016.09.026
10. Zhang Y, Mao X, Su J, et al. Strategy deciphers the underlying molecular mechanisms of qixuehe capsule in the treatment of menstrual disorders. *Chin Med*. 2017;12:23. doi:10.1186/s13020-017-0145-x
11. Zhang S, Shan L, Li Q, et al. Systematic analysis of the multiple bioactivities of green tea through a network pharmacology approach. *Evid Based Complement Alternat Med*. 2014;2014:512081. doi:10.1155/2014/512081
12. Guo W, Huang J, Wang N, et al. Integrating network pharmacology and pharmacological evaluation for deciphering the action mechanism of herbal formula Zuojin Pill in suppressing hepatocellular carcinoma. *Front Pharmacol*. 2019;10:1185. doi:10.3389/fphar.2019.01185
13. Zhao R, Li X, Zhang H, Chen X, Wang Y. Network pharmacology study on the mechanism of gastrodin reversing depressive symptoms in traumatically stressed rats. *Comb Chem High Throughput Screen*. 2022. doi:10.2174/1386207325666220928143206
14. Zhang K. Exploring the Mechanism of Action of Gastrodin against Alzheimer's Disease Based on Network Pharmacology. *Yunnan J Trad Chin Med*. 2022;43 :39–46 doi:10.16254/j.cnki.53-1120/r.2022.09.018.
15. Wei G, Shifeng C, Qibiao S, et al. Antidepressant-like effect of active fraction of polyrhachis vicina roger in a rat depression model. *J Tradit Chin Med*. 2018;38:12–21. doi:10.1016/j.jtcm.2018.02.001
16. Su Q, Su H, Nong Z, et al. Hypouricemic and nephroprotective effects of an active fraction from Polyrhachis vicina roger on potassium oxonate-induced hyperuricemia in rats. *Kidney Blood Press Res*. 2018;43:220–233. doi:10.1159/000487675
17. Liu J, Wei G, Lu W. GC determination of palmitic acid and oleic acid in Poryrhaehis vicina Roger. *Chin J Pharm Anal*. 2016;36:86–90 doi:10.16155/j.0254-1793.2016.01.13.
18. Yan HC, Cao X, Das M, Zhu XH, Gao TM. Behavioral animal models of depression. *Neurosci Bull*. 2010;26:327–337. doi:10.1007/s12264-010-0323-7
19. Abelaira HM, Reus GZ, Quevedo J. Animal models as tools to study the pathophysiology of depression. *Braz J Psychiatry*. 2013;35(Suppl 2):S112–S120. doi:10.1590/1516-4446-2013-1098
20. Gourley SL, Taylor JR. Recapitulation and reversal of a persistent depression-like syndrome in rodents. *Curr Protoc Neurosci*. 2009;9:32.
21. Gourley SL, Kiraly DD, Howell JL, Olausson P, Taylor JR. Acute hippocampal brain-derived neurotrophic factor restores motivational and forced swim performance after corticosterone. *Biol Psychiatry*. 2008;64:884–890. doi:10.1016/j.biopsych.2008.06.016
22. Gourley SL, Wu FJ, Kiraly DD, et al. Regionally specific regulation of Erk Map kinase in a model of antidepressant-sensitive chronic depression. *Biol Psychiatry*. 2008;63:353–359. doi:10.1016/j.biopsych.2007.07.016
23. Thompson SM, Kallarackal AJ, Kvarta MD, Van Dyke AM, LeGates TA, Cai X. An excitatory synapse hypothesis of depression. *Trends Neurosci*. 2015;38:279–294. doi:10.1016/j.tins.2015.03.003
24. Yirmiya R, Rimmerman N, Reshef R. Depression as a microglial disease. *Trends Neurosci*. 2015;38:637–658. doi:10.1016/j.tins.2015.08.001
25. Hodes GE, Kana V, Menard C, Merad M, Russo SJ. Neuroimmune mechanisms of depression. *Nat Neurosci*. 2015;18:1386–1393. doi:10.1038/nn.4113
26. Shu X, Sun Y, Sun X, et al. The effect of fluoxetine on astrocyte autophagy flux and injured mitochondria clearance in a mouse model of depression. *Cell Death Dis*. 2019;10:577. doi:10.1038/s41419-019-1813-9
27. Price RB, Duman R. Neuroplasticity in cognitive and psychological mechanisms of depression: an integrative model. *Mol Psychiatry*. 2020;25:530–543. doi:10.1038/s41380-019-0615-x
28. Yuan L, Zhang J, Guo J-H, et al. Dala2-Gip-Glu-Pal Protects against cognitive deficits and pathology in App/Ps1 Mice by inhibiting neuroinflammation and upregulating Camp/Pka/Creb signaling pathways. *J Alzheimers Dis*. 2021;80(2):695–713. doi:10.3233/JAD-201262
29. Kim YJ, Lee JS, Kim H, Jang JH, Choung YH. Gap junction-mediated intercellular communication of camp prevents cddp-induced ototoxicity via Camp/Pka/Creb pathway. *Int J Mol Sci*. 2021;23:22. doi:10.3390/ijms23010022
30. Gao X, Zhang X, Cui L, et al. Ginsenoside Rb1 promotes motor functional recovery and axonal regeneration in post-stroke mice through Camp/Pka/Creb signaling pathway. *Brain Res Bull*. 2020;154:51–60. doi:10.1016/j.brainresbull.2019.10.006
31. Bibel M, Barde YA. Neurotrophins: key regulators of cell fate and cell shape in the vertebrate nervous system. *Genes Dev*. 2000;14:2919–2937. doi:10.1101/gad.841400
32. Huang EJ, Reichardt LF. Neurotrophins: roles in neuronal development and function. *Annu Rev Neurosci*. 2001;24:677–736. doi:10.1146/annurev.neuro.24.1.677
33. Park H, Poo MM. Neurotrophin regulation of neural circuit development and function. *Nat Rev Neurosci*. 2013;14:7–23. doi:10.1038/nrn3379
34. Esvald EE, Tuvikene J, Sirp A, Patil S, Bramham CR, Timmusk T. Creb family transcription factors are major mediators of BDNF transcriptional autoregulation in cortical neurons. *J Neurosci*. 2020;40:1405–1426. doi:10.1523/JNEUROSCI.0367-19.2019